

Application of HTS Straight Soldered Stack Cable in Subscale Magnet Geometry

D. Sotnikov , D. Araujo , B. Auchmann , M. Duda , C. Lindner, A. Stampfli , and A. Ballarino 

Abstract—High-temperature superconducting (HTS) cables offer a promising opportunity for high-field magnet applications. However, the exact technology stack that would lead to accelerator-quality magnets is as yet not consolidated. A vigorous design-build-test cycle is required to evaluate the potential of different approaches. To implement such program at PSI, in the framework of the CHART initiative, we propose using the same magnet geometry previously tested with an LTS stress-managed magnet while replacing the rectangular Nb₃Sn Rutherford cables with HTS straight soldered stack cables – a design that seamlessly integrates into the existing structure. Currently, we are in the design and process-development stage, with testing planned for later in 2025. This study presents magnetic field-quality estimation and AC loss computations for the HTS common coils magnet, based on finite element method (FEM) modeling of the final magnet design. The study includes an estimation of the required stabilizer content for protection with dump resistor at a maximum applied current of 10 kA, as well as the design of internal and external joints. Additionally, a novel coil-winding technique enables simultaneous winding, insulation, and soldering of the cable, thus, overcoming the tape-stack cable’s low minimal bending radius and offering scalability for larger magnet applications. This work represents a possible way for the practical application of HTS cables in accelerator magnets. A direct benchmark against LTS cables in identical geometry provides valuable insights and a faster path-way to experimental results and model validation.

Index Terms—Superconducting magnets, HTS, superconducting cables.

I. INTRODUCTION

AS PART of the HFM program at CERN [1] and Swiss Accelerator Research and Technology (CHART) program [2], the subscale stress-managed common coil (subSMCC1) magnet based Nb₃Sn produced at PSI and tested in CERN [3]. The subSMCC1 magnet is an important step to achieving 14-T configuration of subscale common-coil magnet SMACC in context of European strategy for Particle Physics Accelerator R&D Roadmap [4]. It was designed to validate the SMCC concept and to test novel technologies, including new

Received 13 October 2025; revised 16 December 2025; accepted 6 January 2026. Date of publication 29 January 2026; date of current version 23 March 2026. This work was supported by the Swiss Accelerator Research and Technology (CHART) program (www.chart.ch). (Corresponding author: D. Sotnikov.)

D. Sotnikov, D. Araujo, M. Duda, C. Lindner, and A. Stampfli are with Paul Scherrer Institut PSI, CH-5234 Villigen, Switzerland (e-mail: dmitry.sotnikov@psi.ch).

B. Auchmann is with Paul Scherrer Institut PSI, CH-5234 Villigen, Switzerland, and also with CERN, CH-1211 Geneva, Switzerland.

A. Ballarino is with CERN, CH-1211 Geneva, Switzerland.

Color versions of one or more figures in this article are available at <https://doi.org/10.1109/TASC.2026.3656860>.

Digital Object Identifier 10.1109/TASC.2026.3656860

processes [5] that could be applied to the next modifications of magnets.

In this work, we chose a more comparative approach by replacing the LTS cable with an HTS cable of straight soldered REBCO tape stack in an existing magnet former from subSMCC1 and called it REBCO subscale version 1 (RS1). For our baseline, we selected a stress-managed LTS magnet using Nb₃Sn Rutherford cables [3], [5] — a design fully developed and fabricated in our laboratory. By duplicating this magnet and simply changing the cable type, we created an ideal setup for a direct performance comparison between superconductors. The selected shape of REBCO tape stack cable allows to use 2D modeling for AC losses estimations, which is simpler than required for transposed cables 3D computations.

This paper includes a brief overview of the final magnet geometry. Since the magnet design copies LTS subscale design that has been presented in detail in previous publications [3] and workshops [7], [8], we only provide a concise description for context.

The production cycle mirrors that of the LTS subscale magnet, with one significant difference: we manufactured the REBCO cable in-house. A custom-built cabling and winding machine was developed. After winding, the coil is positioned in the former, and the cable is soldered using a paste soldering method.

At the time of writing, two racetrack coils have been completed and tested in liquid nitrogen at 77 K. These tests provided valuable data on joint resistance, coil inductance and voltage, protection behavior, and other key parameters used to validate our computational models based on Wellington University database of REBCO tape properties [6]. This data will also inform further evaluations at lower temperatures.

In summary, we have developed and demonstrated a complete production cycle for HTS subscale magnets, from REBCO cable fabrication to final magnet assembly. The coils of 2 layers configuration tested in LN₂ at 77 K. Upcoming tests in liquid helium at 4.5 K will offer insights into the advantages and limitations of REBCO cables compared to Nb₃Sn. Further testing in gaseous helium at 20 K will be used to validate our computational predictions (Table I).

II. DESIGN AND MODELLING

The REBCO-based cable we used is a stack of face-to-face soldered REBCO tapes with pre-tin copper stabilizers soldered together. This configuration corresponds the rectangular cross-section of a Rutherford cable, simplifying manufacturing due to its flat geometry and making it well-suited for racetrack-shaped

TABLE I
COILS PARAMETERS COMPARISON

	HTS 2L RS1	HTS RS1	LTS
Temperature, K	77	4.5	20
I_c , A	500	7890	5600
I_{op} at 85 % of I_c , A	430	7000	5000
Inductance, μ H	375	390	390
Peak field at I_{op} , T	0.28	4.8	3.4
Bore field at I_{op} , T	0.12	3.9	2.8
Energy, kJ	0.036	9.5	4.85

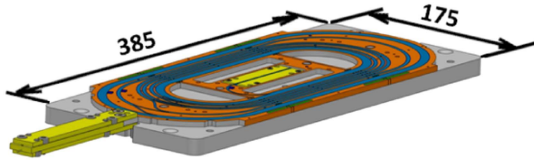


Fig. 1. RS1 single layer coil winding.

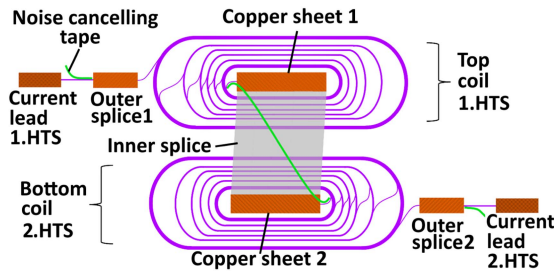


Fig. 2. Schematic picture of 2 layers configuration.

coils. We selected 8 tapes (or 4 of face-to-face soldered tape-stacks) 4-mm width with 20 μ m of copper shell and 40 μ m thickness of Hastelloy in each REBCO tape, that gives 180 μ m of total face-to-face stack. As stabilizer we used 3 strips of 150 μ m copper 4-mm width with about 10 μ of tin-led cover. The total thickness of straight soldered REBCO tape stack cable is about 1.3 mm.

The baseline design for this magnet involves fitting REBCO cables into the former originally used for the LTS subscale magnet [3]. The magnet consists of 4 layers (flat racetracks) with a non-uniform turn distribution. Estimation of the coil parameters during tests are done in 2D FEM model. Each of 4 layers includes 13 meters of insulated REBCO cable wound into a racetrack shape, with gaps between some turns to improve the magnetic field quality (Fig. 1). The racetrack coils are wound in a flat configuration with both central and outer contacts. The design consists of four racetracks, organized into two sets of double coils (Fig. 2), with each set having an inner splice between the two coils.

To estimate the parameters of this coil design, we used 2D FEM simulations (Fig. 3) in COMSOL Multiphysics [9], comparing the results with data from a previously tested LTS coil configuration. Based on induction calculations, which should yield the same values for stationary simulations of the shape, we applied a simple length coefficient of 0.31 m for the magnet. We estimate a critical current (I_c) of 500 A in LN₂, with 430 A corresponding to 85% of I_c . The inductance is expected to

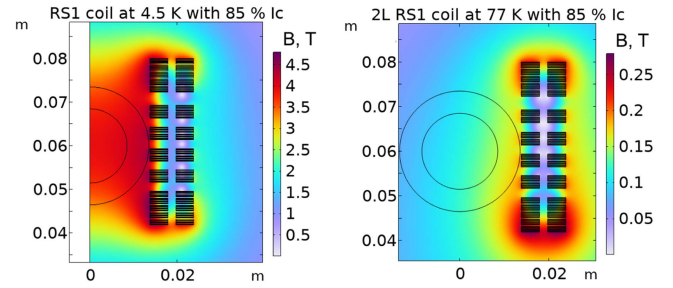


Fig. 3. 2D FEM models for magnetic field of RS1 at 4.5 K (left) and 2 layers RS1 at 77 K (right).

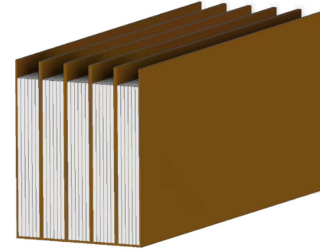


Fig. 4. Straight soldered REBCO tapes stack cable in insulation.

match that of the LTS configuration. That computations done in stationary physics with real $J_c(B, \theta)$ for all REBCO layers for making computations quicker.

Additionally, we calculated the AC losses using 2D FEM transient simulations with the H–A formulation [10] for various operating modes, which we plan to validate in future experiments. The most interesting case is at 20 K, where we have an accurate $J_c(B, \theta)$ dependence. In this scenario, we expect approximately 2 J per cycle at a ramp rate of 10 A/s.

Using long REBCO tape to form the central connection [10] introduces twisting in the region of highest field or requires the tape to pass perpendicularly through the magnetic field—both ways decay critical current and create bottle neck of the coil.

To mitigate these issues, we adopted a double-pancake configuration (Fig. 1), in which both current leads are located in low-field regions. This arrangement minimizes heat input from resistive contacts, avoids field misalignment at central turns, and simplifies manufacturing.

III. PRODUCTION

To simplify and speed up the production process, we chose to use a soldered tape stack as our cable (Fig. 4) and selected commercially available 4-mm face-to-face soldered REBCO tapes from FFJ [11]. This type of REBCO tape has minimum bending radius 10 mm while minimal bending radius of the former is 20 mm.

A. Coil Winding

To implement this configuration, our team developed a custom winding machine capable of handling a stack consisting of four face-to-face soldered 4-mm REBCO cables and three additional pre-tined copper tapes. All tapes are held under tension on

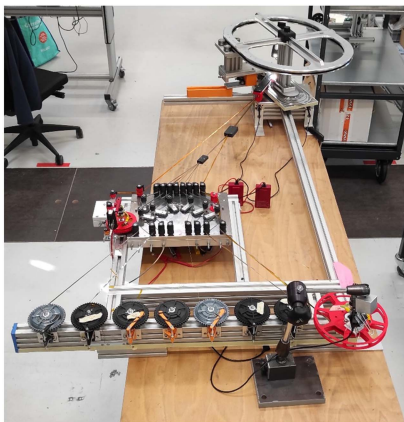


Fig. 5. Racetrack winding machine.

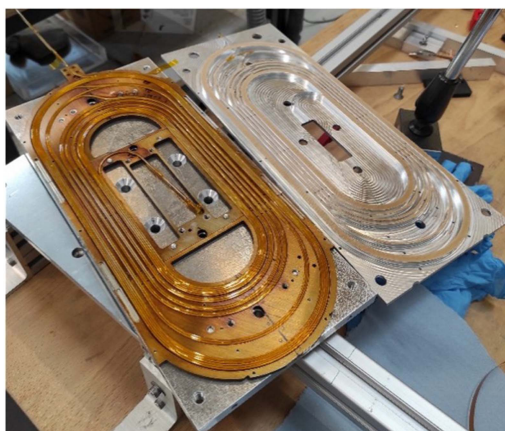


Fig. 6. Winded single RS1 coil in former.

individual spools and guided into a stack using dancers that ensures proper alignment and tension control (Fig. 5). The order of tapes in stack is selected as Stabilizers on edges of stack and one in the middle. In this case we have direct contact of each face-to-face REBCO stack to one of stabilizer layers.

Once the tapes are stacked, they are enclosed in a U-shaped Kapton shell with a thickness of $150\ \mu\text{m}$. This process is continuous. In parallel, the machine also co-winds a $50\ \mu\text{m}$ copper tape, wrapped in $50\ \mu\text{m}$ Kapton insulation. This insulated copper tape is used as a co-winding layer to assist in quench detection, as it follows the exact path of the REBCO cable throughout the winding.

The coil is wound onto a winding tool that replicates the shape of the former. Once winding is complete, the coil is transferred into an insulated former (Fig. 6) using a mechanical pusher.

B. Soldering and Impregnation

After winding, the next step is soldering the stacked tapes into a single, unified cable. The U-shaped insulation design provides top access to the stack, allowing the application of solder paste. Soldering is performed by screwing former to a heat plate with the slots for heater. Temperatures of heat cartridges was $230\ ^\circ\text{C}$, while maximal temperature on former was $210\ ^\circ\text{C}$ and temperature on cables did not exceed $205\ ^\circ\text{C}$.

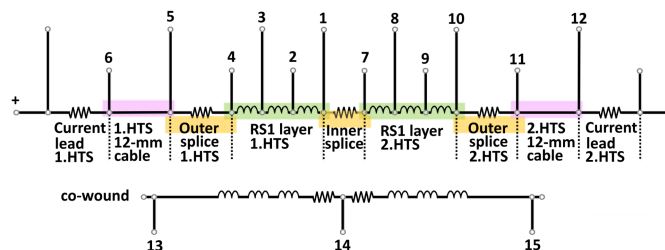


Fig. 7. Test-scheme for 2 L RS1 coil where numbers corresponds to voltage taps.

Voltage taps are soldered into designated pockets on the former. Simultaneously external splices to current leads done through opening face-to-face stack for soldering each 4-mm REBCO tape of stack to 8 of 12-mm REBCO of adaptor cable, that plays role as for prevention of current lead heat dissipation in coil cable – this adapter has 3 times more REBCO layers and it is placed in low field area. This adaptor is a dry stack up to 2 meters long with additionally 0.5 mm thick copper tapes on both sides for cooling and 1 mm thick Teflon strips for mechanical support. Even at high heat income from copper current leads, this heat should not come to the coil. So, all heat can come only through splice between this 12-mm REBCO tape adapter and coil cable.

The coil is impregnated using a wax-based system [12], [13] with the following setup:

- Mold for the wax, with peel sheet for a flat surface finish.
- Cooling and heating plate inside of autoclave.
- Temperature sensors (for heating plate, former and cooling circuit).

The coil is dried overnight. Wax is injected under vacuum when the mold is maintained at $80\text{--}90\ ^\circ\text{C}$. After three vacuum-to-atmosphere cycles, the cooling circuit is activated to solidifying the wax from bottom to top.

C. Coil Assembly

Two impregnated formers are arranged back-to-back. Then an internal splice between two coil layers is made by soldering the cables together at the center, with a 12-mm REBCO tape and copper sheets overlapping both cable ends. The 2-mm gap between the cable was filled with a pretinned copper rod. The copper plates also serve as a cooling surface, as they protrude 9 cm from the splice. This provides both electrical continuity and efficient heat dissipation from splice resistance into the environment. This method selected due to limitation of space for soldering and reproducibility in the next magnets.

IV. TEST AND RESULTS

The coil test was conducted using a two-layer (two-racetrack) configuration 2 L RS1 (scheme is presented in Fig. 7) in liquid nitrogen (LN_2) (Fig. 8). The primary goal of this test was to validate the instrumentation and verify the basic parameters of the coils—most importantly, to confirm that the cable had not been damaged during the production process.

Cooling was performed in a liquid nitrogen bath with direct coolant filling. The coil was energized using a DC power supply, and a varistor was used for protection during the test.

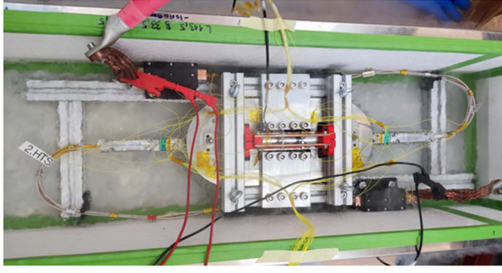


Fig. 8. 2 L RS1 coil in test bath.

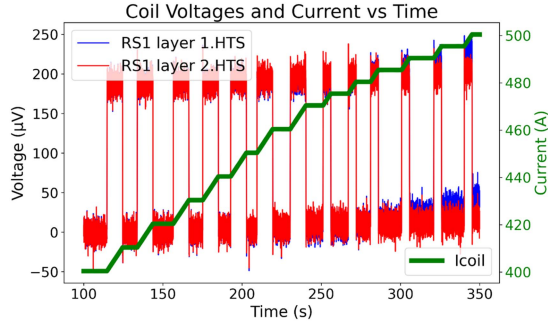


Fig. 9. Voltage on both coils versus current.

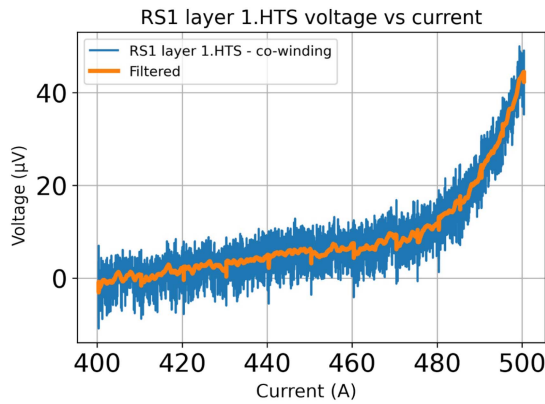


Fig. 10. Voltage increase on 1.HTS coil.

We applied different charging modes to collect as much diagnostic data as possible without risking damage to the coil. All instrumentation signals functioned properly. The co-wound copper tapes for each layer tracked the voltage behavior of their corresponding REBCO coil layers.

To determine the critical current (I_c), the coil was charged in small steps (Fig. 9). Starting at 400 A, the current was increased in 10 A increments at a rate of 1 A/s. From 475 A onward, finer 5 A steps were used at the same rate. A steady voltage rise was observed at approximately 500 A (Fig. 10), indicating the onset of resistive behavior.

Given the 13-meter length of the cable, the I_c criterion was set at 130 μV . However, since the voltage was measured using central taps, a threshold of 50 μV was sufficient to detect the transition.

Among the two HTS coils, only coil 1 (1.HTS) showed a voltage increase near 500 A, suggesting it had reached its critical current. Coil 2 (2.HTS), on the other hand, remained fully

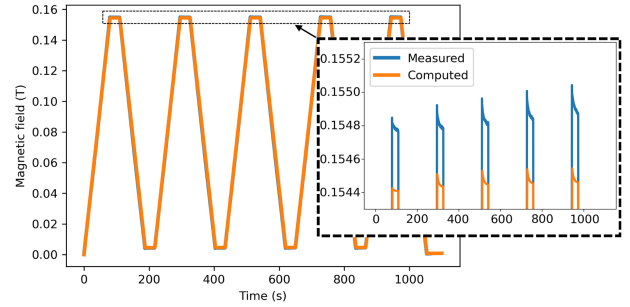


Fig. 11. Hall probe signal in bore of 2 L RS1.

superconducting up to that current. To avoid damaging the coils and to preserve them for further testing at 4.5 K and 20 K, we decided not to increase the current beyond this point. Notably, the critical current remained stable even after several thermal cycles, confirming the coil's robustness.

To validate the simulation model, we also installed a Hall probe sensor in the bore area of the magnet. Since no dedicated slot was prepared, the exact position of the sensor is unknown. However, we were able to estimate its location and align it with the simulated field distribution for comparison (see Fig. 11). The simulation model returned magnetic field values closely matched to measured results. Most interesting, the magnetization of computations showed the same trend as gotten by experiment, confirming the consistency between the computed and measured data.

We also measured the resistance of the splices: the inner splice showed a resistance of approximately 260 $\text{n}\Omega$, while the outer splices were below 60 $\text{n}\Omega$. These measurements will aid in modeling and predicting full coil behavior during future tests at 20 K and 4.5 K.

V. CONCLUSION

At PSI, development is underway on the ReBCO Subscale (RS1) magnet—an advanced stress-managed common coil magnet based on the well-established stress-management concept. This approach was previously implemented in the subSMCC1 magnet and is currently being further refined in the asymmetric common-coil configuration at PSI, the RS1 project extends this methodology to ReBCO-based systems. The RS1 magnet will be tested over a variable temperature range from 4.5 K (for straight comparison with gotten previously data of Nb_3Sn cable for LTS subscale magnet [3]) and 20 K (for validation of models with experimentally gotten $J_c(B, \theta)$ from University of Wellington database of REBCO tapes [6]) and will include integrated auxiliary coils to support ESC-based quench protection strategies in accordance with subSMCC magnet.

Initial testing has begun with half of the superconducting assembly, consisting of two spliced ReBCO racetrack coils in a stress-managed layout. These coils were operated in liquid nitrogen (LN_2), reaching their predicted short-sample current limit without any observable degradation in critical current (I_c) after multiple thermal cycles. These successful early tests validate the integrity of the coil fabrication process and provide a strong foundation for the upcoming low-temperature evaluations.

REFERENCES

- [1] B. Auchmann, "High field magnet programme–European strategy input," Workshop, CERN, Geneva, Switzerland, pp. 3–4, Mar. 31, 2025.
- [2] CHART MagDev at PSI. Accessed: Oct. 13, 2025. [Online]. Available: <https://www.psi.ch/en/cas/chart-magdev>
- [3] D. Araujo et al., "Manufacturing and testing of the first Nb₃Sn subscale stress-managed common-coils: 2-in-1 dipole magnet developed at the paul scherrer institute," *IEEE Trans. Appl. Supercond.*, vol. 35, no. 5, Aug. 2025, Art. no. 4002807, doi: [10.1109/TASC.2025.3533392](https://doi.org/10.1109/TASC.2025.3533392).
- [4] CERN, "European strategy for particle physics accelerator R&D roadmap: Report from the LDG," CERN, Geneva, Switzerland, Dec. 8, 2024.
- [5] D. Araujo et al., "Subscale stress-managed common coil design," *IEEE Trans. Appl. Supercond.*, vol. 34, no. 5, Aug. 2024, Art. no. 4003905, doi: [10.1109/TASC.2024.3360220](https://doi.org/10.1109/TASC.2024.3360220).
- [6] High-temperature superconducting wire critical current database. Accessed: Oct. 13, 2025. [Online]. Available: <https://htsdb.wimbush.eu/dataset/13708690>
- [7] T. Michlmayer, "Updates to manufacturing processes on subscale SM-CC," presentation in workgroup "Common-Coils", CERN, Geneva, Switzerland, Apr. 19, 2024.
- [8] D. Araujo, "Progress on the PSI subscale stress-managed common-coils SMCC," presentation in workgroup "Common-Coils", CERN, Geneva, Switzerland, Jun. 19, 2024.
- [9] Comsol Multiphysics software. Accessed: Oct. 13, 2025. [Online]. Available: <https://www.comsol.com/>
- [10] J. Xiaoyu, "The improved model based on the H-A formulation in large-scale HTS magnet," *Supercond. Sci. Technol.*, vol. 618, Mar. 2024, Art. no. 1354431, doi: [10.1016/j.physc.2024.1354498](https://doi.org/10.1016/j.physc.2024.1354498).
- [11] Faraday Factory Japan, Product. Accessed: Oct. 13, 2025. [Online]. Available: <https://www.faradaygroup.com/en/product/>
- [12] A. Brem, "From hot to cold: Advanced materials and processes for Nb₃Sn based magnets," *IEEE Trans. Appl. Supercond.*, vol. 34, no. 5, Aug. 2024, Art. no. 7700105, doi: [10.1109/TASC.2023.3338588](https://doi.org/10.1109/TASC.2023.3338588).
- [13] A. Stampfli, "PSI SMACC1 design review: Impregnation procedure and electrical integrity," in *Proc. PSI SMACC1 Des. Rev. Workshop*, Villigen, Switzerland, Jan. 14, 2025, pp. 2–8.